J. Fluid Mech. (2014), *vol.* 761, *pp.* 105–122. © Cambridge University Press 2014
doi:10.1017/jfm.2014.635

Multiple states for flow through a collapsible tube with discontinuities

A. Siviglia[1,†] **and M. Toffolon**[2]

[1]Laboratory of Hydraulics, Hydrology and Glaciology (VAW), ETH Zurich, 8093 Zurich, Switzerland

[2]Department of Civil, Environmental and Mechanical Engineering, University of Trento, 38123 Trento, Italy

(Received 28 March 2014; revised 20 October 2014; accepted 28 October 2014; first published online 14 November 2014)

We study the occurrence of the multiple steady states that flows in a collapsible tube can develop under the effect of: (i) geometrical alterations (e.g. stenosis), (ii) variations of the mechanical properties of the tube wall, or (iii) variations of the external pressure acting on the conduit. Specifically, if the approaching flow is supercritical, two steady flow states are possible in a restricted region of the parameter space: one of these flow states is wholly supercritical while the other produces an elastic jump that is located upstream of the variation. In the latter case the flow undergoes a transition through critical conditions in the modified segment of the conduit. Both states being possible, the actual state is determined by the past history of the system, and the parameter values show a hysteretic behaviour when shifting from one state to the other. First we set up the problem in a theoretical framework assuming stationary conditions, and then we analyse the dynamics numerically in a one-dimensional framework. Theoretical considerations suggest that the existence of multiple states is associated with non-uniqueness of the steady-state solution, which is confirmed by numerical simulations of the fully unsteady problem.

Key words: biological fluid dynamics, flow–vessel interactions, shallow water flows

1. Introduction

The human body is permeated by flexible tubes that transport different kinds of biological fluids such as blood, air, lymph, cerebrospinal fluid and urine (Skalak, O'zkaya & Skalak 1989; Grotberg 1994; Ku 1997; Grotberg & Jensen 2004). Almost all the conduits transporting such fluids can be treated as passive elastic tubes (Bertram 2004) in which interactions between the pressure of the fluid and compliant walls determine velocity profiles and wall displacement patterns (Heil & Hazel 2011). Some biological tubes work under distended conditions (e.g. arteries; Downing & Ku 1997), i.e. the cross-section is circular and the internal pressure is higher than the external pressure. Conversely, there are other biological tubes for which the external pressure is higher than the internal one (Shapiro 1977). Then, as in the case of veins, the tube collapses to a flattened cross-section where the flow continues through it, but the available cross-sectional area diminishes dramatically (Bertram 2004).

† Email address for correspondence: siviglia@vaw.baug.ethz.ch

It is the complexity of the fluid–structure interactions that gives collapsible tubes their specific dynamic features. Among them, flow limitations and self-excited oscillations are the most peculiar. Choking occurs when a smooth transition connects a subcritical to a supercritical flow. In this case a flow limitation occurs: given the conditions upstream of the point where the flow becomes critical, there is a maximum flow rate that the tube can convey independently of the difference between upstream and downstream pressures (Shapiro 1977). This phenomenon is clearly visible during forced expiration, when the maximal air outflow rate from the lung is independent of the effort put forward by the patient: it is noteworthy that this phenomenon has been modelled successfully within a one-dimensional framework (Elad, Kamm & Shapiro 1987, 1988). Self-excited oscillations occur in externally pressurized collapsible tubes. In a classical experimental framework, used to mimic physiological systems (e.g. Bertram, Raymond & Pedley 1990, 1991), a segment of floppy conduit is mounted between two rigid tubes and enclosed inside a pressurized chamber. Several types of unsteady behaviour are detected from the experiment, such as highly nonlinear oscillations and hysteresis between the transition among different oscillatory regimes. Also in this case, various hypotheses have been formulated by means of simple one-dimensional models to explain the genesis of self-excited oscillations (e.g. Jensen 1990; Hayashi, Hayase & Kawamura 1998), but the current challenge of theoretical work is towards a better representation of reality (Bertram 2004). Other analyses suggest the possible existence of multiple steady flow states in collapsible tubes (Kececioglu *et al.* 1981; Reyn 1987), which is the topic of this paper.

In a one-dimensional framework, the equations for the flow in collapsible tubes are formally identical to those governing open channel flows (e.g. Shapiro 1977; Kamm & Shapiro 1979; Pedley 2000). However, the closure for the pressure is more complex and contains additional parameters (external pressure, stiffness, exponents of the tube law), thus introducing a higher degree of complexity in the analysis of the flow in collapsible tubes. A few studies have exploited the analogy between the two systems to transfer some results obtained in the simpler case of open channel flows. A first example is the development of roll waves that occur under supercritical conditions. This aspect has been analysed by Brook, Falle & Pedley (1999), who investigated numerically the circumstances under which roll waves form, develop and propagate in collapsible tubes. A second example concerns the existence of multiple solutions of the Riemann problem when geometrical discontinuities are present in a open channel flow (Bernetti, Titarev & Toro 2007) or in collapsible tubes (Toro & Siviglia 2013).

Another interesting phenomenon that has received attention in open channel flows is the occurrence of the multiple states that the flow over a long obstacle can develop within a certain range of parameters. In particular, two different locally steady flow states are possible as a function of the Froude number, and the actual solution depends on the manner in which the flow is established (that is, its history), thus leading to a hysteretic behaviour. This phenomenon has been described by means of analytical theories (Baines 1984), laboratory experiments (Baines & Davies 1980; Baines 1984) and numerical investigations (Pratt 1983). The aim of this paper is to study this problem in the context of collapsible tubes, which may lead to a peculiar behaviour in biological processes. Thus, we develop an analytical theory and carry out numerical simulations to identify the conditions under which this hysteretic behaviour is possible for variations of the geometrical (i.e. stenosis) and mechanical (i.e. stiffer or softer material) properties of the conduit, and of the external pressure. In particular, we seek the solution in terms of the speed index S (Shapiro 1977) of the undisturbed approaching flow: this dimensionless parameter represents the ratio between the flow

velocity and the celerity of the small perturbations and controls the flow conditions (subcritical $S < 1$, supercritical $S > 1$).

The structure of the paper is the following. In § 2 we introduce the governing equations of the one-dimensional mathematical model and the closure relationships. In § 3 we develop a theoretical approach to describe the bistable region in the parameter space assuming stationary conditions. Finally, in § 4 we perform some numerical experiments in unsteady conditions to test the dynamic behaviour of the system. Conclusions are addressed in § 5.

2. Formulation of the problem

The one-dimensional equations governing the flow in collapsible tubes are the usual continuity and momentum equations

$$\frac{\partial A}{\partial t} + \frac{\partial Q}{\partial x} = 0, \tag{2.1}$$

$$\frac{\partial Q}{\partial t} + \frac{\partial}{\partial x}(uQ) + \frac{A}{\rho}\frac{\partial p}{\partial x} = -Ru, \tag{2.2}$$

where t is time, x is the longitudinal axis, and $R = 8\pi\mu/\rho$ is the flow resistance in the case of a laminar flow, with μ and ρ the dynamic viscosity and the density of the fluid, respectively. The cross-sectional area of the elastic tube is A, the flow rate is Q, the velocity is $u = Q/A$ and the internal pressure is p. Dealing with collapsible tubes, we assume the tube law

$$p = p_e + K(\alpha^m - \alpha^{-n}), \tag{2.3}$$

where p_e is the external pressure, the coefficient K describes the elastic properties of the vessel, $\alpha = A/A_0$ is the area ratio, with A_0 the reference area for which $p = p_e$, and m and n are positive coefficients. For the analysis developed in § 3, we assume $R = 0$ in order to derive simpler analytical relationships.

Two boundary conditions are to be imposed to determine the actual flow field. The direction along which their influence is transferred depends on the celerity c of small elastic perturbations with respect to flow velocity. This information is provided by the speed index

$$S = \frac{u}{c}, \tag{2.4}$$

which is the analogue of the Froude number in open channel flows. In order to have a well-posed problem, the first boundary condition is always set at the inlet of the tube (in terms of the flow rate Q or an analogous quantity), while the position of the second boundary condition is fixed either at the inlet (for a supercritical flow, $S > 1$) or at the outlet (for a subcritical flow, $S < 1$). For the tube law (2.3), the speed index can be calculated by means of the relationship

$$S^2 = \frac{\rho Q^2}{KA_0^2\alpha^2(m\alpha^m + n\alpha^{-n})}. \tag{2.5}$$

Siviglia & Toffolon (2013) showed that there is another dimensionless parameter controlling the properties of the flow in collapsible tubes. This parameter emerges

$\boldsymbol{V}$	$\boldsymbol{F}$
A	$Q = uA$
u	$\mathscr{P} = \frac{u^2}{2} + \frac{p}{\rho}$
$Q = uA$	$\mathscr{M} = u^2 A + \frac{p}{\rho} A - \frac{1}{\rho} \int p \, \mathrm{d}A$

TABLE 1. The first three cases of the general equation (2.7) for the flow in collapsible tubes with constant parameters K, A_0 and p_e.

from the non-dimensionalization of the governing equations (2.1) and (2.2), as demonstrated in appendix A. It reads

$$\chi = \frac{K A_0^2}{\rho Q_0^2}, \tag{2.6}$$

where Q_0 is a reference flow rate.

Adapting the analysis of Whitham (1974) of open channel flows to (2.1) and (2.2), it is possible to demonstrate that an infinite number of equations in the form

$$\frac{\partial \boldsymbol{V}(u, A)}{\partial t} + \frac{\partial \boldsymbol{F}(u, A)}{\partial x} = 0 \tag{2.7}$$

can be derived in this ideal frictionless case. The most important equations are reported in table 1: it is easy to recognize that the flux $\boldsymbol{F}$ is given by the flow rate Q in the first case, i.e. (2.1), the total pressure $\mathscr{P}$ (also known as stagnation pressure, divided by ρ in this definition) in the second case, and the momentum flux $\mathscr{M}$ (divided by ρ also in this case) in the third case, corresponding to the conservative form of (2.2). Note that if p is also an explicit function of x and not only of $A(x)$, because of the variation of A_0, K or p_e, the momentum flux is not conserved and additional source terms have to be included in (2.7), as shown for instance by Brook *et al.* (1999). Other conservation equations can be derived by solving the two coupled equations

$$\frac{\partial \boldsymbol{F}}{\partial u} = u \frac{\partial \boldsymbol{V}}{\partial u} + A \frac{\partial \boldsymbol{V}}{\partial A} \quad \text{and} \quad \frac{\partial \boldsymbol{F}}{\partial A} = \frac{1}{\rho} \frac{\partial p}{\partial A} \frac{\partial \boldsymbol{V}}{\partial u} + u \frac{\partial \boldsymbol{V}}{\partial A}. \tag{2.8a,b}$$

We refer to Whitham (1974) for the procedure to derive such relationships.

3. Steady state: theoretical approach

Siviglia & Toffolon (2013) illustrated how variations of the geometrical or mechanical properties can produce a transition through critical conditions (i.e. $S = 1$) in both subcritical and supercritical flows for steady-state problems. In the present analysis, we demonstrate that a bistable configuration (with two alternative solutions whose occurrence depends on the history of the system) exists in the supercritical region of the parameter space, similarly to what has been shown for open channel flows (Baines & Davies 1980; Pratt 1983; Baines 1984, 1995). In order to identify the bistable region, we consider steady-state frictionless conditions. When variations

of the parameters A_0, K or p_e are considered, $\boldsymbol{F}$ is not always conserved in (2.7). In particular, Q and $\mathscr{M}$, which for the tube law (2.3) reads

$$\mathscr{M} = u^2 A + \frac{KA}{\rho}\left(\frac{m}{1+m}\alpha^m + \frac{n}{1-n}\alpha^{-n}\right), \tag{3.1}$$

are conserved across stationary discontinuities of A (elastic jumps) if the parameters are constant, while Q and $\mathscr{P}$ are conserved if A varies continuously also when the parameters vary. In the first case, some energy is lost in the sudden expansion of the flow, eventually dissipated by viscosity in a process that is analogous to that occurring in hydraulic jumps. Consistently with the assumption of perfectly elastic walls, no energy loss takes place in the tube wall (Cowley 1982).

Referring to the sketch in figure 1 for the case of a reference supercritical flow ($S > 1$) as upstream boundary condition, we analyse two different configurations: (i) a flow that remains supercritical while passing smoothly through a modified section (with variation of A_0, K or p_e); and (ii) a transcritical flow for which an elastic jump forms upstream of the modified region. We define the sections (a)–(c) as in figure 1: a smooth passage always occurs from (b) to (c), while a sudden change of area occurs from (a) to (b) in the transcritical configuration. Such a jump can move upstream or downstream, so we assume steady-state conditions in a reference frame moving with the speed c_f of front propagation (assumed positive downstream).

For a subcritical flow ($S < 1$), the elastic jump will form in the downstream region, with sections (a)–(c) defined symmetrically with respect to the modified region. However, bistable states do not exist in this case, as will be demonstrated below.

3.1. *General equations including the case of an elastic jump*

For both subcritical and supercritical flows, introducing the tube law (2.3) we can write the conservation equations (of flow rate and momentum flux in the moving frame) between sections (a) and (b) as

$$(u_a - c_f)A_a = (u_b - c_f)A_b, \tag{3.2}$$

$$\left[(u_a - c_f)^2 + \frac{K}{\rho}\left(\frac{m}{m+1}\alpha_a^m - \frac{n}{n-1}\alpha_a^{-n}\right)\right]A_a = \left[(u_b - c_f)^2 + \frac{K}{\rho}\left(\frac{m}{m+1}\alpha_b^m - \frac{n}{n-1}\alpha_b^{-n}\right)\right]A_b, \tag{3.3}$$

and the conservation equations (of flow rate and total pressure) between sections (b) and (c) as

$$u_b A_b = u_c A_c, \tag{3.4}$$

$$\frac{u_b^2}{2} + \frac{p_e}{\rho} + \frac{K}{\rho}(\alpha_b^m - \alpha_b^{-n}) = \frac{u_c^2}{2} + \frac{p_{ec}}{\rho} + \frac{K_c}{\rho}(\alpha_c^m - \alpha_c^{-n}), \tag{3.5}$$

where $\alpha_c = A_c/A_{0c}$, and p_{ec} is the external pressure in section (c). Equation (3.3) is also known as the Rankine–Hugoniot condition and (3.5) represents the Riemann invariant preservation (e.g. Toro & Siviglia 2013). When no transition through critical conditions occurs, no elastic jump exists, and we can simply set the equalities

$$u_a = u_b, \quad A_a = A_b, \tag{3.6a,b}$$

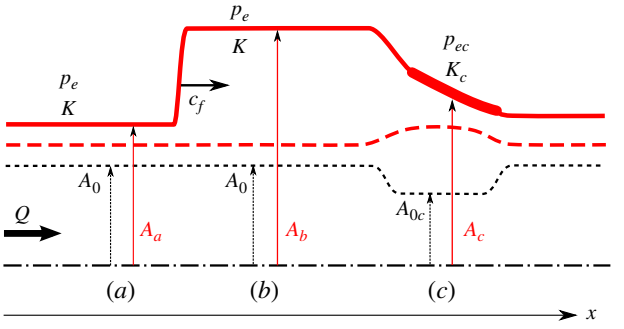

FIGURE 1. (Colour online) Sketch of a longitudinal section of half-tube and corresponding notation: the thick solid grey line (red online) represents the vessel configuration when an elastic jump is present, and the thick dashed grey line (red online) that when no transition occurs. Three locations are identified and used in the text (with reference to a supercritical flow, $S > 1$): (a) upstream boundary condition, (b) section with the possible presence of an elastic jump travelling with a celerity c_f, and (c) region with modified external pressure (p_{ec}), geometrical (A_{0c}) and mechanical (K_c) properties, where critical conditions may occur.

instead of (3.2) and (3.3), implying that Q is constant in both time and space. It is worth noting that equations (3.6) represent a trivial solution of equations (3.2) and (3.3), which hence represent the general formulation of the problem that can always be described by the four equations (3.2)–(3.5).

We can now impose the upstream boundary conditions u_a and A_a (or, equivalently, χ and α_a in dimensionless form) and study the possible solutions. In the case without transition, $c_f = 0$ obviously, and the four unknowns (u_b, A_b, u_c and A_c) can be obtained in a simple way exploiting relations (3.6) and reducing the problem to two equations and two unknowns (u_c and A_c).

On the other hand, the case of transcritical flow with an elastic jump contains five unknowns (u_b, A_b, u_c, A_c and c_f) and hence one degree of freedom. However, critical flow conditions (i.e. $S = 1$) occur in the modified section (c) when the elastic jump forms because the transition from subcritical to supercritical is located there (see Siviglia & Toffolon (2013) for further details), yielding the additional equation

$$\frac{\rho u_c^2}{K_c(m\alpha_c^m + n\alpha_c^{-n})} = 1, \tag{3.7}$$

and closing the system.

It is worth making the problem dimensionless in order to highlight the parameters controlling the solution. We introduce the definitions

$$\kappa = \frac{K_c}{K}, \quad \delta = \frac{A_{0c}}{A_0}, \quad \eta = \frac{p_{ec} - p_e}{K}, \quad \sigma = \frac{c_f}{Q/A_0}, \tag{3.8a–d}$$

where K and A_0 refer to the unmodified part of the tube (sections (a) and (b), see figure 1). Reducing the four equations to two by solving (3.2) and (3.4) for u_b and u_c, we obtain

$$\alpha_b^m - \alpha_b^{-n} + \frac{1}{2\chi\alpha_b^2}[1 + \sigma(\alpha_b - \alpha_a)]^2 = \kappa(\alpha_c^m - \alpha_c^{-n}) + \eta + \frac{1}{2\chi\delta^2\alpha_c^2}[1 + \sigma(\alpha_b - \alpha_a)]^2 \tag{3.9}$$

from (3.5) and

$$\frac{(\alpha_b-\alpha_a)(1-\sigma\alpha_a)^2}{\chi\alpha_a\alpha_b}=\frac{m}{m+1}(\alpha_b^{m+1}-\alpha_a^{m+1})-\frac{n}{n-1}(\alpha_b^{-n+1}-\alpha_a^{-n+1}) \tag{3.10}$$

from (3.3). It is easy to see that $\alpha_b=\alpha_a$ is the trivial solution of (3.10) corresponding to the absence of an elastic jump.

In addition, the critical condition (3.7) for the transcritical case reads

$$[1+\sigma(\alpha_b-\alpha_a)]^2=\chi\kappa\delta^2\alpha_c^2(m\alpha_c^m+n\alpha_c^{-n}). \tag{3.11}$$

Moreover, the speed index can be expressed as a function of the dimensionless boundary conditions (α_a, χ) by

$$S^2=\frac{1}{\chi\alpha_a^2(m\alpha_a^m+n\alpha_a^{-n})}. \tag{3.12}$$

3.2. *Marginal surfaces and the bistable region in the parameter space*

In order to analyse the multiple states of the system and delimit the region of the parameter space where they can occur, we define two different surfaces in the space defined by the variables χ, α_a, δ, κ and η. The first surface is identified by the solution of (3.9) with $\alpha_b=\alpha_a$ and the critical condition (3.11), which represents the limit for the existence of a flow state without transition through critical conditions. The second surface is delimited by the marginal condition $\sigma=0$, which characterizes a steady elastic jump. Both surfaces can be determined by solving the following equations:

$$\alpha_b^m-\alpha_b^{-n}+\frac{1}{2\chi\alpha_b^2}=\kappa(\alpha_c^m-\alpha_c^{-n})+\eta+\frac{1}{2\chi\delta^2\alpha_c^2}, \tag{3.13}$$

$$\frac{(\alpha_b-\alpha_a)}{\chi\alpha_a\alpha_b}=\frac{m}{m+1}(\alpha_b^{m+1}-\alpha_a^{m+1})-\frac{n}{n-1}(\alpha_b^{-n+1}-\alpha_a^{-n+1}), \tag{3.14}$$

$$1=\chi\kappa\,\delta^2\alpha_c^2(m\,\alpha_c^m+n\,\alpha_c^{-n}). \tag{3.15}$$

Note that the two surfaces in the parameter space are determined on the basis of the two families of solutions of (3.14): (i) the trivial solution $\alpha_b=\alpha_a$, and (ii) the solution that considers the presence of the elastic jump ($\alpha_b\neq\alpha_a$).

For assigned values of χ and α_a, a solution of the system (3.13)–(3.15) can be obtained for the two unknowns (α_b and α_c) and for one of the modified parameters (δ, κ or η) while fixing the other two. This allows one to plot the marginal curves and define the regions in a two-parameter space. In this case, the solution of the system (3.13)–(3.15) identifies two curves in the parameter space: (i) the transcritical curve ($\alpha_b=\alpha_a$ with $S(\alpha_c)=1$), and (ii) the curve for a stationary elastic jump (i.e. $\sigma=0$). Figure 2 shows an example of these two marginal curves considering variations of δ, κ and η (independently) as a function of the boundary condition expressed in terms of α_a (*a–c*) or $S(\alpha_a)$ (*d–f*), for a given value of χ, with $m=0.5$ and $n=0$. We will demonstrate below that: (i) in the region delimited by the transcritical curve, all flow states must pass through critical conditions in section (*c*), thus producing an elastic jump; and (ii) the elastic jump tends to move far away from section (*c*) within the region delimited by curve obtained for $\sigma=0$. As a consequence, we will show that the shaded region of figure 2 is the bistable region, and that multiple states exist only for supercritical flows.

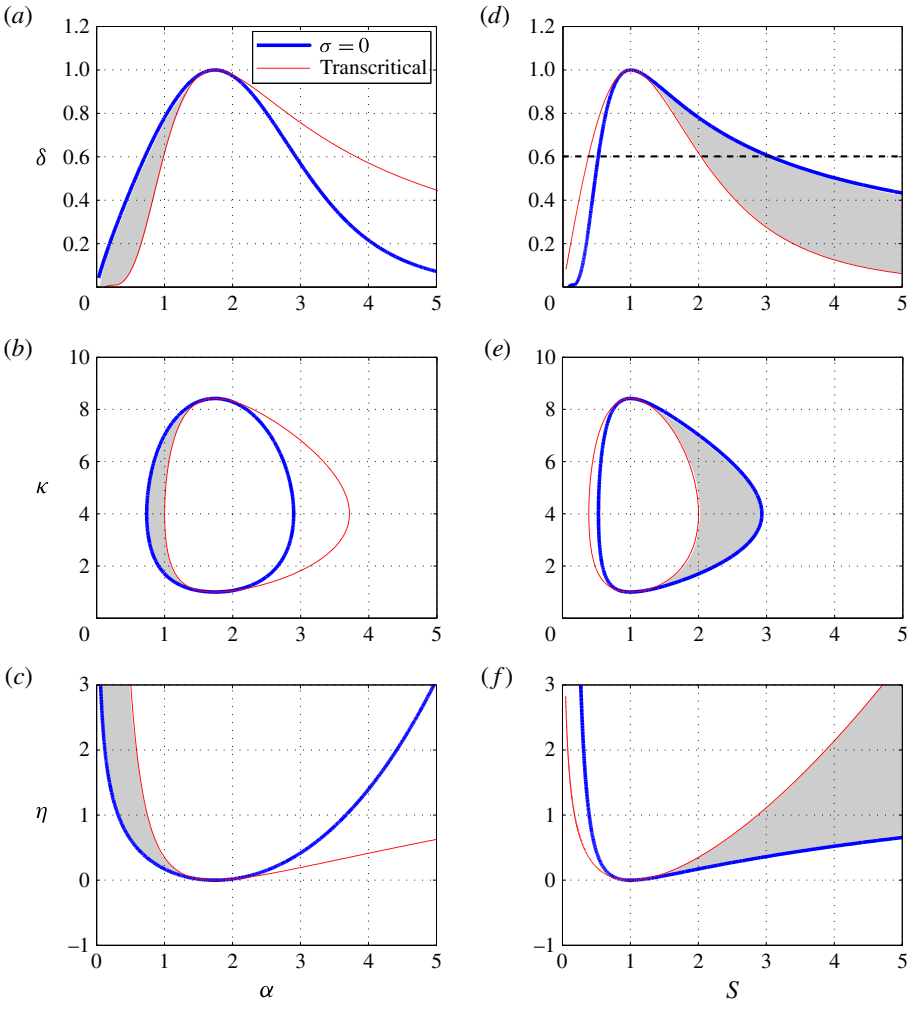

FIGURE 2. (Colour online) Bistable region (shaded) defined by the marginal curve for transcritical conditions and the curve for a steady elastic jump ($\sigma = 0$) in different parameter spaces, as a function of $\alpha \equiv \alpha_a$ (*a–c*) and S (*d–f*) and for $\chi = 0.5$, $m = 0.5$ and $n = 0$ ($\chi_{ce} = 2$) in the case of variations of: (*a*,*d*) the reference area δ ($\kappa = 1$, $\eta = 0$), (*b*,*e*) the mechanical properties of the tube κ ($\delta = 1$, $\eta = 0$), and (*c*,*f*) the external pressure η ($\delta = 1$, $\kappa = 1$). All variables are dimensionless. The horizontal dashed line at $\delta = 0.6$ in (*d*) represents the section examined in figure 3.

In order to understand how the flow conditions change in the different regions, we examine the details of the solution along one section of figure 2(*d*), identified by the dashed line, as a function of $S(\alpha_a)$. Hence we fix all the parameters (i.e. $\delta = 0.6$, $\kappa = 1$ and $\eta = 0$) and one of the two boundary conditions ($\chi = 0.5$, which can be seen as the dimensionless flow rate): figure 3 shows the solution of the system as a function of the other boundary condition $S(\alpha_a)$. We can now describe the interplay between the necessary condition for the onset of the elastic jump and the condition for its enduring presence in the system.

Assuming that no transition occurs (i.e. no elastic jump, thus $\alpha_b = \alpha_a$), (3.10) is automatically satisfied and the solution α_c can be obtained from (3.9). Figure 3(*a*)

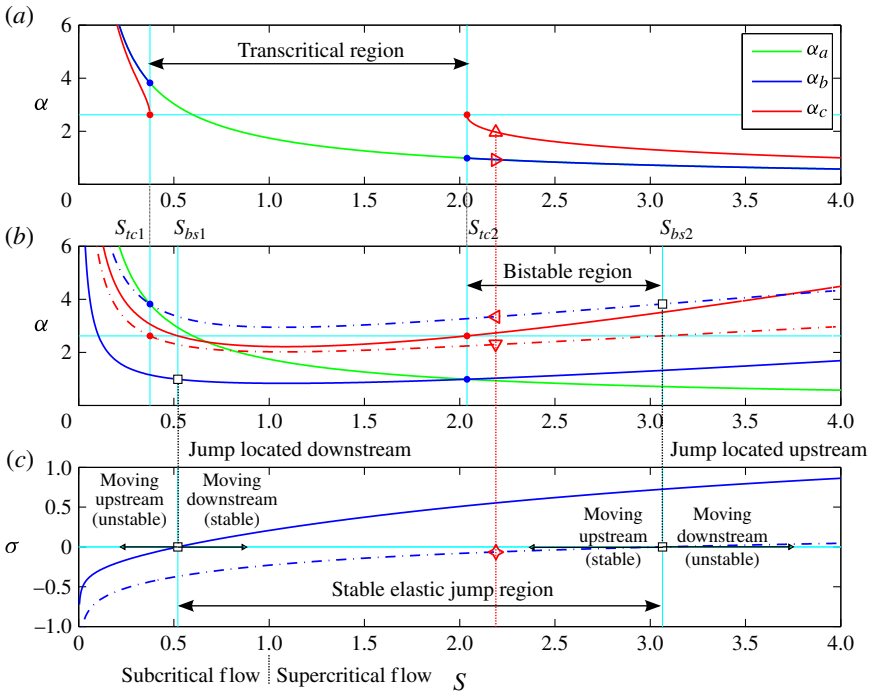

FIGURE 3. (Colour online) The solution for the relative area ratios α_b and α_c in the case of: (*a*) absence of the elastic jump (thus $\alpha_b = \alpha_a$ when possible), and (*b*) for an elastic jump moving with dimensionless front speed σ (*c*), as a function of $S(\alpha_a)$ for $\chi = 0.5$, $\delta = 0.6$, $\kappa = 1$, $\eta = 0$, $m = \frac{1}{2}$ and $n = 0$. Dots in (*a*,*b*) indicate the limits of the transcritical region. Squares in (*b*,*c*) indicate the limits of the region in which the elastic jump, identified by the relative area α_b ($\neq \alpha_a$), tends to go away from the obstacle, thus sustaining its own existence. Solid and dashed lines in these panels indicate the two possible solutions with the elastic jump, which can be located either upstream (when $S > 1$) or downstream ($S < 1$) of the obstacle. Triangles orientated with different directions in (*a*,*b*) identify the flow conditions highlighted in figure 5(*a*) ($S = 2.2$); the four-pointed star in (*c*) identifies the front speed in the same figure.

shows the behaviour as a function of S: it clearly appears that the solution $\alpha_b = \alpha_a$ exists only outside of the so-called transcritical region delimited by two values of S_{tc} ($S < S_{tc1}$ and $S > S_{tc2}$, where subscript *tc* stands for transcritical). We refer to Siviglia & Toffolon (2013) for a deeper analysis of this case. Conversely, an elastic jump forms for all values of S within the transcritical region ($S_{tc1} < S < S_{tc2}$): this is a necessary condition since no solution exists that does not pass through critical conditions in the modified region (*c*). However, the elastic jump can exist also outside the transcritical region, but its front will not, in general, be stationary. The solution with the presence of a moving elastic jump is investigated in the following paragraph.

The solution of the equations (3.9)–(3.11), accounting for a moving elastic jump and critical conditions in section (*c*), is shown in figure 3(*b*), with the dimensionless speed σ of the jump plotted in figure 3(*c*). In this case two different configurations are possible (indicated with solid and dashed lines, respectively): a jump located downstream of the obstacle (i.e. section (*c*) of the tube) for subcritical flow ($S < 1$) and upstream of it for supercritical flows ($S > 1$). A special case is that of the

steady elastic jump ($\sigma = 0$): we can consequently identify three regions delimited by two characteristic values of S (S_{bs1} and S_{bs2}, where subscript bs stands for bistable). Looking at the signs of the front speed, we can argue that the elastic jump tends to go away from the obstacle that produced it in the region $S_{bs1} < S < S_{bs2}$. For instance, in supercritical conditions the jump is located upstream and its speed is negative (thus moving it further upstream) for values of $S < S_{bs2}$. In this case, if the jump is produced in the transcritical region, it will stably remain in the system also for values of S outside such a region. On the other hand, for $S > S_{bs2}$ the elastic jump is moving downstream ($\sigma > 0$, i.e. towards the obstacle) and will tend to disappear unless it is not re-created in the transcritical region ($S_{tc1} < S < S_{tc2}$). Therefore, a bistable region can be identified for supercritical flows in the region $S_{tc2} < S < S_{bs2}$: here, if the solution is smooth (wholly supercritical) it will remain such, while if a transition with an elastic jump is somehow produced, it will not disappear. For the sake of clarity, we note that in figure 3 the bistable region is defined by the range $2 \lesssim S \lesssim 3$ approximately.

On the other hand, in subcritical conditions the elastic jump is located downstream of the obstacle, and the region in which it will move away from the obstacle (i.e. further downstream, $\sigma > 0$) is for $S > S_{bs1}$. However, since $S_{bs1} > S_{tc1}$, this region is already included in the transcritical region. Conversely, for $S < S_{tc1}$ the elastic jump is always moving upstream ($\sigma < 0$), thus precluding its persistent existence outside of the transcritical region where it is formed. This implies that multiple solutions do not exist in the subcritical case.

It is worth noting that the extent of the bistable region, which is quite large in figure 2, actually depends on the value of χ and of the tube law parameters m and n. Using for instance different values, highly nonlinear, such as those that have been used for veins (e.g. Brook *et al.* 1999; Müller & Toro 2014), i.e. $m = 10$ and $n = 1.5$, the shape of the marginal curves and of the bistable region changes significantly (figure 4). Moreover, the location and the area of the curves in the parameter space depends on the difference between χ and $\chi_{ce} = (m + n)^{-1}$ (Siviglia & Toffolon 2013), and is especially evident for variations of κ. When $\chi > \chi_{ce}$, as in figure 2, the transcritical region is centred on values of $\alpha > 1$ and draws a closed region in the semi-plane $\kappa > 1$, thus defining an upper boundary. When $\chi < \chi_{ce}$, as in figure 4, the region is centred on $\alpha < 1$ and transition occurs in the range $\kappa = 0$–1. Finally, we note that only positive values of the excess of external pressure ($\eta > 0$) can induce transcritical conditions, and hence the presence of the bistable region, when the other alterations are not present.

4. Numerical experiments

Numerical experiments have been performed in order to analyse the bistable behaviour of the solution identified in the previous section. We developed a code that numerically solves the system of governing equations (2.1) and (2.2), including the friction term and using the mathematical approach described in Toro & Siviglia (2013). The numerical solution is then obtained using the finite volume method of the path-conservative type developed by Müller & Toro (2013), which is first-order accurate.

We consider in particular the effect of a stenosis inducing a transition in a supercritical flow. Thus, we consider a segment of a collapsible tube, characterized by homogeneous mechanical properties (uniform K) and external pressure (uniform p_e), with a local variation of the geometrical reference area A_0. We note that this is

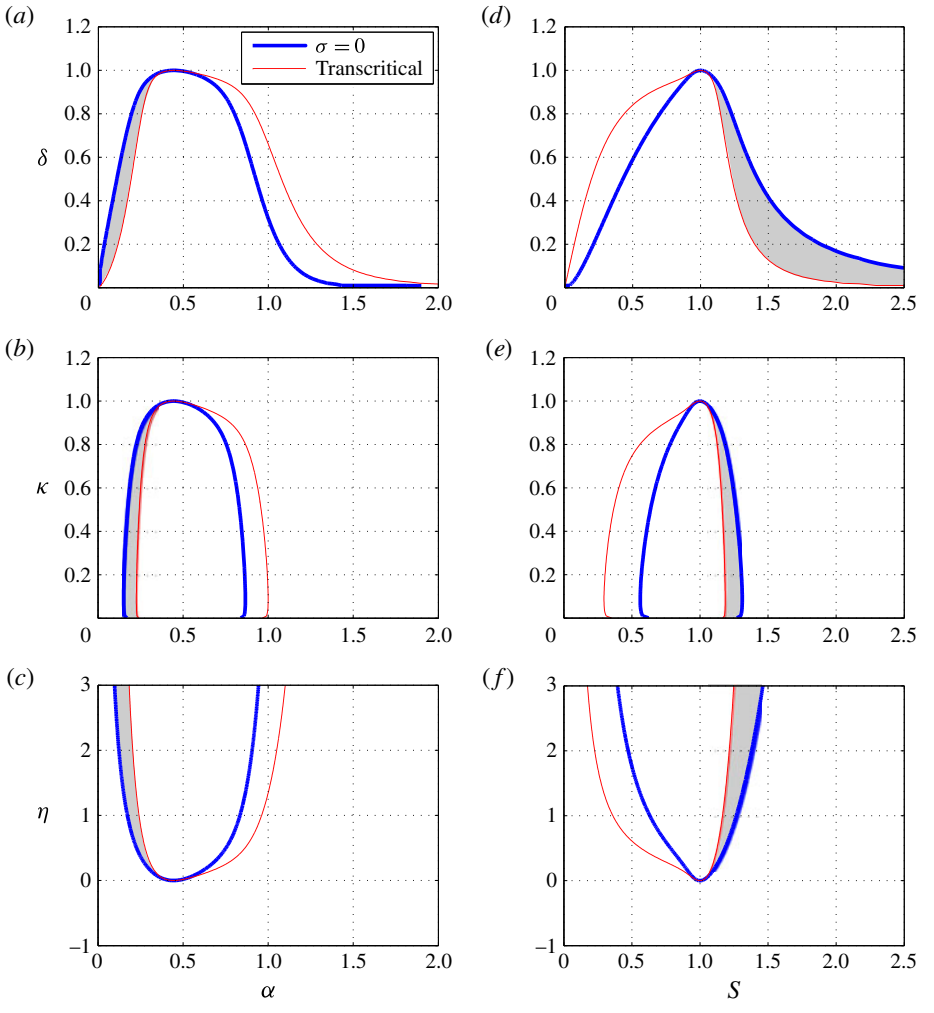

FIGURE 4. (Colour online) Bistable region (shaded) in the same plots as in figure 2, but for $\chi = 1$, $m = 10$ and $n = 1.5$ ($\chi_{ce} = 0.087$).

only one of the possible configurations. In fact, similar analyses can be performed for mechanical variations (i.e. local change of K) or for alterations of the external pressure p_e: the general analysis discussed in § 3 provides in any case a theoretical background to interpret the results of these cases.

Focusing on the case of a local variation of A_0 and referring to the undisturbed value of A_0 to identify the intrinsic scale, we describe a stenosis by means of the dimensionless equation

$$\delta(x^*) = 1 - \lambda \sin^2 \left[\pi \left(\frac{x^* - x_1^*}{x_2^* - x_1^*} \right) \right], \tag{4.1}$$

where λ is the maximum reduction factor and $x^* = x/D$ is defined as in appendix A. For the numerical experiment, we choose $\lambda = 0.4$ (hence $\delta = 0.6$) to analyse the same case as in figure 3. The tube has a nominal diameter $D = 6.0$ mm and a length $L = 3D$,

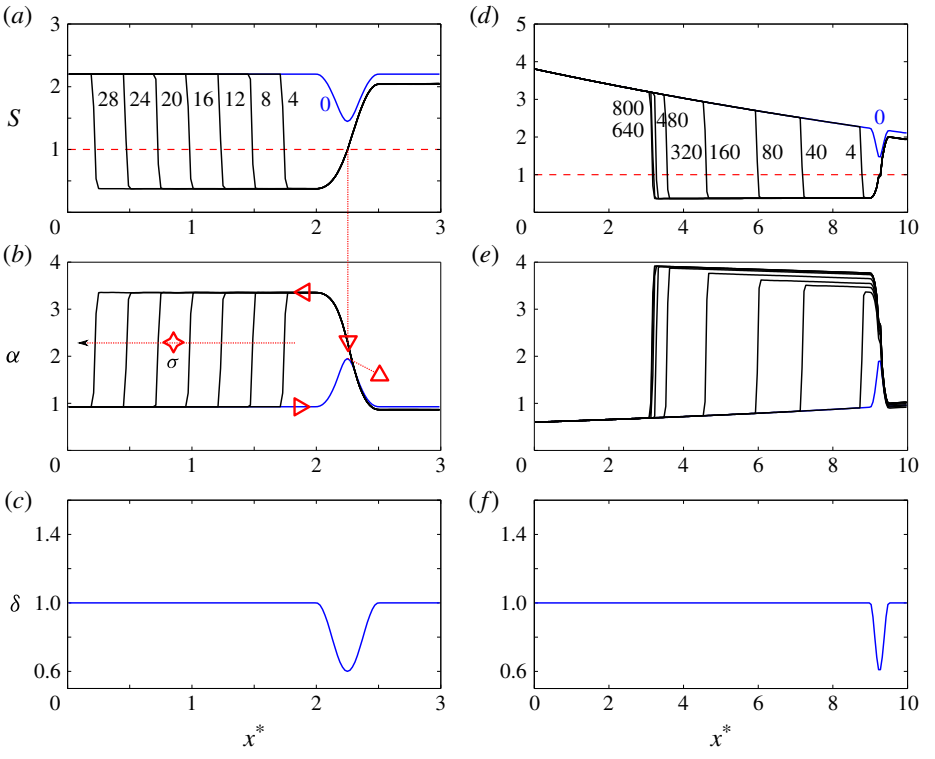

FIGURE 5. (Colour online) Alternative flow configurations in a uniform tube with a stenosis as in (4.1), for $\chi = 0.5$, $m = 0.5$ and $n = 0$. The speed index S (*a*), the dimensionless area α (*b*) and the variation of the reference area δ (*c*) are shown for the frictionless case. Labels in (*a*) indicate the dimensionless times $t^* = t/T$, with T defined as in appendix A. Triangles with different orientations refer to the flow conditions determined in figure 3, as well as the four-pointed star representing the speed of the elastic jump. The effect of considering friction is shown in (*d–f*) considering a longer domain.

and we locate the stenosis between $x_1^* = 2$ and $x_2^* = 2.5$. The tube law is described by $m = 0.5$ and $n = 0$, with $K = 125$ Pa and $p_e = 0$. The fluid density is $\rho = 1050$ kg m^{-3}. Since we reproduce an undisturbed supercritical flow, both boundary conditions are set at the inlet: we impose $\chi = 0.5$ (which fixes the flow rate Q) and $S = 2.2$ (which provides the value of α and hence p).

For the numerical solution, we assume at the outlet transparent (or transmissive) boundaries. This is achieved numerically by imposing boundary conditions that allow the passage of waves without any effect on them. The domain is described by 150 cells and numerical stability is enforced imposing a Courant–Friedrichs–Lewy number $CFL = 0.95$.

Figure 5 illustrates the dynamics of the bistable solution in the frictionless case ($R = 0$, see figure 5*a–c*). The curves labelled with 0 in panels (*a*) and (*b*) show the steady state of the flow conditions expressed in terms of S and α. The speed index of the undisturbed flow is $S = 2.2$, which is in the bistable region shaded in figure 2(*d*) ($\delta = 0.6$, $\chi = 0.5$). Hence, two different configurations are theoretically possible. In this initial setting, the flow does not show any transition through critical conditions and would indefinitely maintain this state if the system is not perturbed.

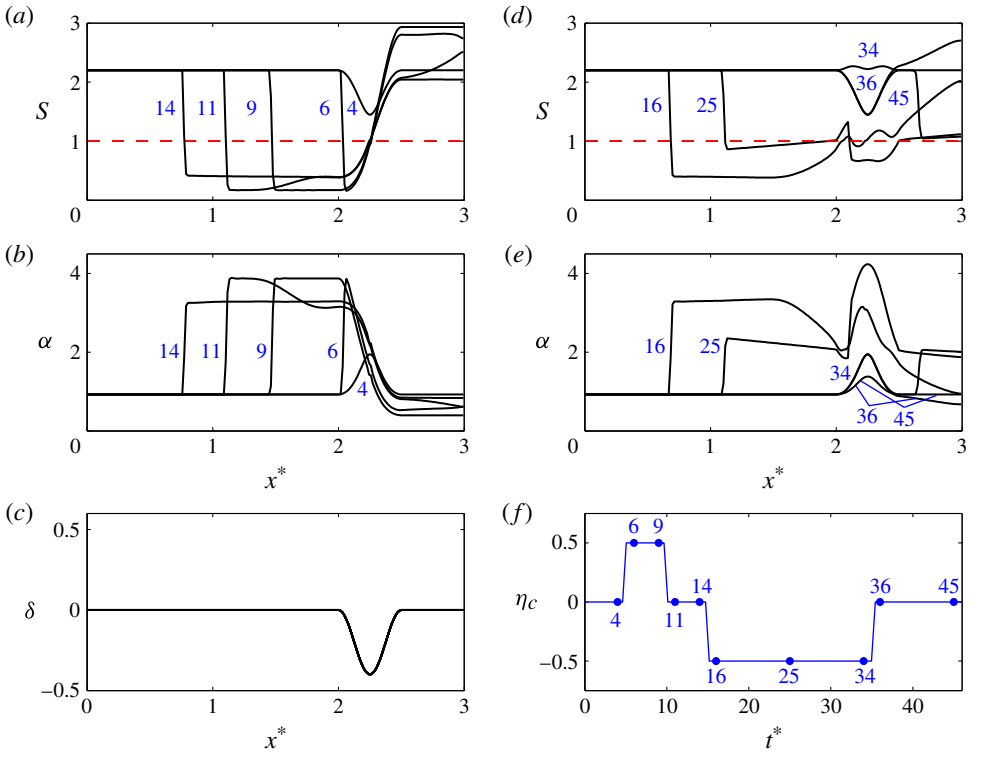

FIGURE 6. (Colour online) Hysteretic behaviour produced by a variation of the dimensionless external pressure η_c in the section with a stenosis (f). The sequence of flow states is indicated by numbers reporting dimensionless times as in (f): the speed index S (a,d), the dimensionless area α (b,e) and the variation of the reference area δ (c,f) are shown for the frictionless case with $\chi = 0.5$, $m = 0.5$ and $n = 0$.

In order to produce the transition to the alternative state, we impose a sudden increase of external pressure $\eta = 0.5$ in the region of the stenosis, and then restore the initial value after a short time (0.02 s, corresponding to 1.6 dimensionless time units). As a consequence of the perturbation, the system shifts to the second alternative state, characterized by an elastic jump propagating upstream. The evolution is depicted in figure 5(a) (where labels refer to the dimensionless time $t^* = t/T$): the elastic jump moves, producing local subcritical conditions ($S < 1$, a necessary condition to have an upstream movement) without being deformed and with a constant speed σ. It is worth noting that the flow conditions of this frictionless case are exactly predicted within the theoretical framework of § 3. The values of α indicated by triangles with different orientations in figure 5(b) correspond to the same symbols in figure 3(a) (initial state without transcritical flow) and figure 3(b) (migrating elastic jump). Moreover, the speed of the elastic jump is correctly estimated by the value of σ in figure 3(c) (see the four-pointed star).

Interestingly, a further perturbation of the external pressure (with an opposite sign with respect to the one that produced the elastic jump) may be able to restore the initial wholly supercritical state (figure 6). As a consequence, it is possible to create a periodic shift between the two alternative states, whereby the flow conditions oscillate following a hysteresis cycle. The actual occurrence of this hysteretic behaviour

depends on both the intensity of the perturbation and the timing, but its existence can be easily predicted on the basis of the theoretical framework proposed in § 3.

The undisturbed upstream migration of the elastic jump is obviously possible only in the idealized frictionless case. In the real world, friction is always present, though, and it is necessary to understand the implications of the energy dissipation on the flow field. Figure 5(*d–f*) shows the effect of introducing the friction term R, which has been evaluated using a dynamic viscosity $\mu = 4 \times 10^{-3}$ Pa s, in (2.2). In order to illustrate the complete dynamics, a much longer domain has been adopted for this specific case ($L = 10D$). As in the analysis of the previous case, the line labelled with 0 indicates the steady state, which is characterized by variations of S and α due to the total pressure drop along the tube. The upstream boundary condition has been set, imposing different values of S (but the same $\chi = 0.5$) to obtain $S \simeq 2.2$ just upstream of the stenosis, with the aim to have a fair comparison with the frictionless case. Similarly to that case, also in the new setting the shift to the alternative flow state (with transcritical flow conditions) is produced by the same temporary alteration of the external pressure. As a consequence, the elastic jump starts moving upstream with a speed that is initially very similar to that of the frictionless case, and reduces only at a relatively long distance from the stenosis (and for a much longer time, as indicated by the labels on the curves). Differently from the frictionless case, if energy dissipation is considered the elastic jump stops; this occurs when the momentum flux is balanced by the local flow conditions (which change along the tube), and eventually a stationary condition is reached. It is important to recognize that the effect of friction depends on the velocity. As can be noted by figure 5(*d*), the variation of S is mild in the subcritical region of the elastic jump, where the velocity is lower than in the undisturbed part of the tube. Therefore, the influence of friction on the transcritical flow caused by the stenosis is virtually negligible in many cases, thus supporting the frictionless theoretical framework developed in § 3.

However, the unaltered propagation of the elastic jump in the frictionless case (or the long displacement necessary to reach the stationary condition in the frictional case) poses the relevant question of understanding what happens within a finite-length collapsible tube. In this case the bistable elastic jump travelling in the upstream direction may interact with internal boundary conditions such as variations of the tube properties, junctions or confluences. In order to illustrate these effects, we consider a sequence of two segments in a domain of length $L = 3D$ and we impose a change of A_0 at a distance $x^* = 1$ from the inlet. The downstream segment (where the stenosis is located) is chosen to be representative of the reference values, and the values of the parameters in the upstream segment is varied accordingly. We consider two cases: a narrowing (figure 7*c*) and a widening (figure 7*f*).

For the sake of clarity in the analysis, we focus on the frictionless case and impose an upstream boundary condition that produces $S = 2.2$ in the part of the tube with the stenosis (see figure 7*a*,*d*). As in the standard case, a transcritical flow is triggered by the temporary variation of external pressure and the system shifts towards the second state. Hence, the elastic jump propagates upstream until it reaches the modified upstream segment. In the case of downstream narrowing (i.e. the migrating jump experiences a widening), the elastic jump is able to pass through (figure 7*b*) the geometrical discontinuity because the momentum flux of the elastic jump is higher than the momentum flux of the flow corresponding to the narrowing. An acceleration of its speed can be noticed (see the time labels in figure 7*a*). In the absence of friction, the elastic jump will continue the migration indefinitely.

The case of downstream widening (i.e. a narrowing for the migrating jump) is more complex, because the propagation of the elastic jump is stopped (figure 7*d*) and a

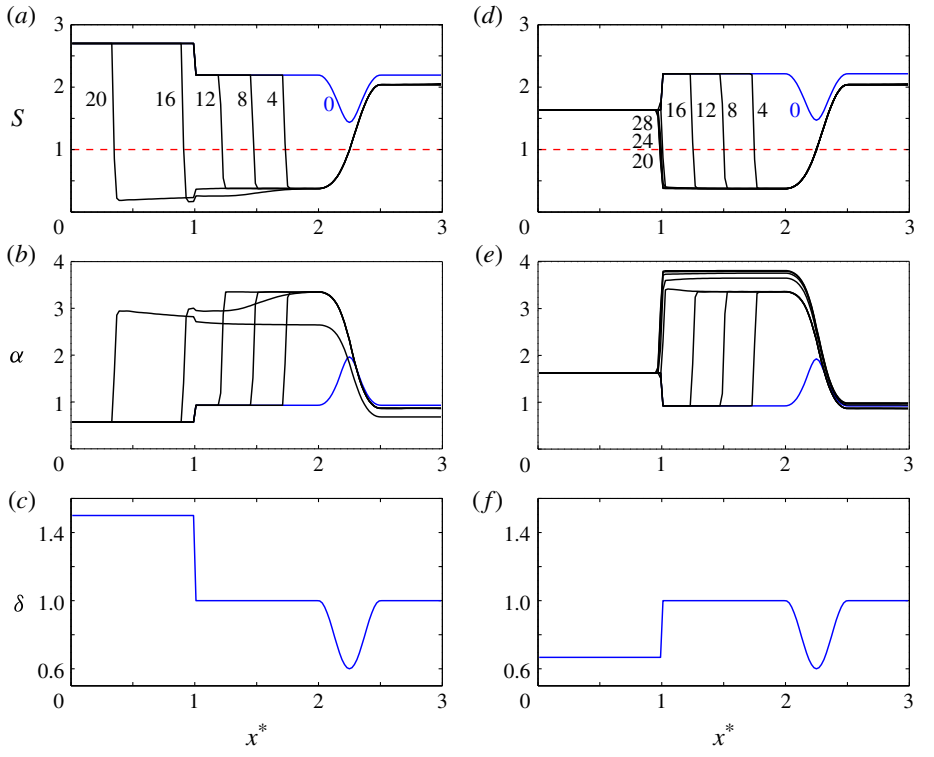

FIGURE 7. (Colour online) Alternative flow conditions for a sequence of two tube segments with variation of the reference area A_0 (the dimensionless variable δ is reported in (*c*) for a narrowing and in (*f*) for a widening), for $\chi = 0.5$, $m = 0.5$ and $n = 0$. The speed index S (*a*,*d*), the dimensionless area α (*b*,*e*) and the variation of the reference area δ (*c*,*f*) are shown for the frictionless case. Labels in (*a*,*d*) indicate the dimensionless times $t^* = t/T$.

reflected wave is generated between the internal boundary condition and the stenosis, producing another type of stationary condition. The small variation of the value of α (figure 7*e*) is caused by the fact that the flow rate becomes uniform along the whole tube when the steady state is reached everywhere. The inclusion of friction does not alter the picture unless the distance between the stenosis and the transition between the tube segments is long enough to significantly change the hydrodynamic conditions of the local flow or of the elastic jump.

5. Conclusions

We have presented an analytical theory to predict the conditions for the occurrence of multiple flow states in collapsible tubes. In fact, two alternative states (so that we term the corresponding region in the parameter space as 'bistable') can exist for a range of values of the speed index S bordering on the transcritical values identified by Siviglia & Toffolon (2013): one solution is smooth and without transition through critical conditions, which are defined by $S = 1$, while the other is characterized by the presence of an elastic jump, which always develops when the flow is forced to pass from super- to subcritical conditions. The occurrence of these multiple solutions

can be triggered by variations in the conduit that can be thought of as local obstacles, like the presence of geometrical alterations (i.e. stenoses), variations of mechanical properties of the tube wall, or variations of the external pressure.

In order to delimit the bistable region, we analytically derived the two marginal curves that are defined by: (i) the condition for which a smooth flow (i.e. without transition) becomes critical when passing through the obstacle (this condition defines the 'transcritical' region as in Siviglia & Toffolon (2013)), and (ii) the condition for which the elastic jump, which develops within the transcritical region, is not moving. Such a bistable region exists only for supercritical flows ($S > 1$), when the elastic jump is located upstream of the obstacle and the propagation of its front is directed upstream outside of the transcritical region. Since the latter condition does not occur for $S < 1$ (where the front forms downstream of the obstacle and should move further downstream in order to remain in the system when outside of the transcritical region), no bistable region exists for subcritical flows.

We exploited the theoretical relationships to investigate a wide range of conditions in terms of the dimensionless number χ, defined by (2.6), of the dimensionless area ratio α (or equivalently the speed index S), and of the dimensionless parameters describing the obstacle (δ, κ, η). Thus we were able to determine the extent of the bistable region, which depends crucially on the exponents of the tube law. The hysteretic behaviour is more likely to occur in compliant tubes such as the veins, in which waves travel slowly and the fluid flow speed may reach and overcome the reduced wave speed and supercritical conditions may occur (Pedley, Brook & Seymour 1996; Bertram 2004).

While the theoretical analysis was conducted by assuming steady-state conditions, we investigated the dynamic behaviour of the system by means of a numerical model. Numerical results confirm the predictions of the analytical theory, showing that in supercritical flow conditions a temporary perturbation (for instance of the external pressure acting on the tube) is sufficient to make the solution shift between the two steady states predicted by the theory. We performed different numerical experiments. In two runs we considered a collapsible tube characterized by constant wall mechanical properties and a stenosis. We showed that the bistable elastic jump (triggered by a perturbation of external pressure) travels indefinitely upstream in the inviscid case, while it stops at certain distance upstream from the stenosis if frictional losses are taken into account. In other two runs we investigated the inviscid propagation of the bistable elastic jump within a collapsible tube of finite length. The results show that the upstream migration of the elastic jump can be stopped by the presence of an internal boundary condition (between tube segments with different geometrical or mechanical properties) imposing flow conditions for which the momentum flux is higher than the one associated with the approaching elastic jump. This eventually produces a steady configuration characterized by a stable immobile elastic jump located at the transition between the tube segments. Conversely, if the momentum flux characterizing the bistable elastic jump has a larger value than the one imposed by the internal boundary condition, the elastic jump can pass through and propagate indefinitely further upstream. The presence of friction losses spatially limits this propagation.

The existence of alternating states with elastic jumps and smooth flows, and the possible effects of the hysteretic behaviour on the physiology of human beings and animals (e.g. the giraffe, see Pedley *et al.* (1996)) are still waiting for proper investigation.

Appendix A. Dimensionless formulation for a tube with uniform properties

If the geometrical (A_0) and mechanical (K) properties do not change, the frictionless problem can be cast in dimensionless form by introducing the following scaling:

$$Q = Q^* Q_0, \quad x = x^* D, \quad t = t^* T, \quad \{p, p_e\} = \{p^*, p_e^*\} K, \tag{A 1a–d}$$

where $D = 2\sqrt{A_0/\pi}$ is a nominal diameter of the tube, Q_0 is a reference flow rate, $T = DA_0/Q_0$ is the time scale chosen to respect the balance in the continuity equation, and * denotes dimensionless variables. Thus, (2.1)–(2.3) become

$$\frac{\partial \alpha}{\partial t^*} + \frac{\partial Q^*}{\partial x^*} = 0, \tag{A 2}$$

$$\frac{\partial Q^*}{\partial t^*} + \frac{\partial}{\partial x^*}\left(\frac{Q^{*2}}{\alpha}\right) + \chi\, \alpha \frac{\partial p^*}{\partial x^*} = 0, \tag{A 3}$$

$$p^* = p_e^* + (\alpha^m - \alpha^{-n}), \tag{A 4}$$

and the problem is characterized by the single dimensionless parameter χ.

REFERENCES

BAINES, P. G. 1984 A unified description of two-layer flow over topography. *J. Fluid Mech.* **146**, 127–167.

BAINES, P. G. 1995 *Topographic Effects in Stratified Flows*. Cambridge University Press.

BAINES, P. G. & DAVIES, P. A. 1980 Laboratory studies of topographic effects in rotating and/or stratified fluids. In *Orographic Effects in Planetary Flows*, chap. 8, pp. 233–299. GARP Publication no. 23, WMO/ICSU.

BERNETTI, R., TITAREV, V. A. & TORO, E. F. 2007 Exact solution of the Riemann problem for the shallow water equations with discontinuous bottom geometry. *J. Comput. Phys.* **227** (6), 3212–3243.

BERTRAM, C. D. 2004 Flow phenomena in floppy tubes. *Contemp. Phys.* **45** (1), 45–60.

BERTRAM, C. D., RAYMOND, C. J. & PEDLEY, T. J. 1990 Mapping of instabilities during flow through collapsed tubes of different length. *J. Fluids Struct.* **4**, 125–153.

BERTRAM, C. D., RAYMOND, C. J. & PEDLEY, T. J. 1991 Application of nonlinear dynamics concepts to the analysis of self-excited oscillations of a collapsible tube conveying a fluid. *J. Fluids Struct.* **5**, 391–426.

BROOK, B. S., FALLE, S. A. E. G. & PEDLEY, T. J. 1999 Numerical solutions for unsteady gravity-driven flows in collapsible tubes: evolution and roll-wave instability of a steady state. *J. Fluid Mech.* **396**, 223–256.

COWLEY, S. J. 1982 Elastic jumps on fluid-filled elastic tubes. *J. Fluid Mech.* **116**, 459–473.

DOWNING, J. M. & KU, D. N. 1997 Effects of frictional losses and pulsatile flow on the collapse of stenotic arteries. *Trans. ASME: J. Biomech. Engng* **119**, 317–324.

ELAD, D., KAMM, R. D. & SHAPIRO, A. H. 1987 Choking phenomena in a lung-like model. *Trans. ASME: J. Biomech. Engng* **109**, 1–92.

ELAD, D., KAMM, R. D. & SHAPIRO, A. H. 1988 Mathematical simulation of forced expiration. *J. Appl. Physiol.* **65**, 14–25.

GROTBERG, J. B. 1994 Pulmonary flow and transport phenomena. *Annu. Rev. Fluid Mech.* **26**, 529–571.

GROTBERG, J. B. & JENSEN, O. E. 2004 Biofluid mechanics in flexible tubes. *Annu. Rev. Fluid Mech.* **36**, 121–147.

HAYASHI, S., HAYASE, T. & KAWAMURA, H. 1998 Numerical analysis for stability and self-excited oscillation in collapsible tube flow. *Trans. ASME: J. Biomech. Engng* **120** (4), 468–475.

HEIL, M. & HAZEL, A. L. 2011 Fluid–structure interaction in internal physiological flows. *Annu. Rev. Fluid Mech.* **43**, 141–162.

JENSEN, O. E. 1990 Instabilities of flow in a collapsed tube. *J. Fluid Mech.* **220**, 623–659.

KAMM, R. D. & SHAPIRO, A. H. 1979 Unsteady flow in a collapsible tube subjected to external pressure or body forces. *J. Fluid Mech.* **95**, 1–78.

KECECIOGLU, I., MCCLURKEN, M. E., KAMM, R. & SHAPIRO, A. H. 1981 Steady, supercritical flow in collapsible tubes. Part 1. Experimental observations. *J. Fluid Mech.* **109**, 367–389.

KU, D. N. 1997 Blood flow in arteries. *Annu. Rev. Fluid Mech.* **29**, 399–434.

MÜLLER, L. O. & TORO, E. F. 2013 Well-balanced high-order solver for blood flow in networks of vessels with variable properties. *Intl J. Numer. Meth. Biomed. Engng* **29** (12), 1388–1411.

MÜLLER, L. O. & TORO, E. F. 2014 A global multi-scale mathematical model for the human circulation with emphasis on the venous system. *Intl J. Numer. Meth. Biomed. Engng* **30** (7), 681–725.

PEDLEY, T. J. 2000 Blood flow in arteries and veins. In *Perspectives in Fluid Dynamics* (ed. G. K. Batchelor, H. K. Moffat & M. G. Worster), pp. 105–158. Cambridge University Press.

PEDLEY, T. J., BROOK, B. S. & SEYMOUR, R. S. 1996 Blood pressure and flow rate in the giraffe jugular vein. *Phil. Trans. R. Soc. Lond.* B **351**, 855–866.

PRATT, L. J. 1983 A note on nonlinear flow over obstacles. *Geophys. Astrophys. Fluid Dyn.* **24**, 63–68.

REYN, J. W. 1987 Multiple solutions and flow limitation for steady flow through a collapsible tube held open at the ends. *J. Fluid Mech.* **174**, 467–493.

SHAPIRO, A. H. 1977 Steady flow in collapsible tubes. *Trans. ASME: J. Biomech. Engng* **99**, 126–147.

SIVIGLIA, A. & TOFFOLON, M. 2013 Steady analysis of transcritical flows in collapsible tubes with discontinuous mechanical properties: implications for arteries and veins. *J. Fluid Mech.* **736**, 195–215.

SKALAK, P., O'ZKAYA, N. & SKALAK, T. C. 1989 Biofluid mechanics. *Annu. Rev. Fluid Mech.* **21**, 167–204.

TORO, E. F. & SIVIGLIA, A. 2013 Flow in collapsible tubes with discontinuous mechanical properties: mathematical model and exact solutions. *Commun. Comput. Phys.* **13** (2), 361–385.

WHITHAM, G. B. 1974 *Linear and Nonlinear Waves*. Wiley.